ELSEVIER

Dipolar cross-relaxation modulates signal amplitudes in the ^{1}H NMR spectrum of hyperpolarized [^{13}C]formate

Matthew E. Merritt [a,b,*], Crystal Harrison [a,d], William Mander [f],
Craig R. Malloy [a,b,c,g], A. Dean Sherry [a,b,e]

[a] *Advanced Imaging Research Center, University of Texas Southwestern Medical Center, Dallas, TX 75390-8568, USA*
[b] *Department of Radiology, University of Texas Southwestern Medical Center, Dallas, TX 75390-8568, USA*
[c] *Department of Internal Medicine, University of Texas Southwestern Medical Center, Dallas, TX 75390-8568, USA*
[d] *Department of Physics, The University of Texas at Dallas, Richardson, TX 75080-3021, USA*
[e] *Department of Chemistry, The University of Texas at Dallas, Richardson, TX 75080-3021, USA*
[f] *Oxford Instruments Molecular Biotools, Tubney Woods, Abingdon, Oxfordshire OX13 5QX, UK*
[g] *VA North Texas Healthcare System, Dallas, TX 75216-7167, USA*

Abstract

The asymmetry in the doublet of a spin coupled to hyperpolarized ^{13}C has been used previously to measure the initial polarization of ^{13}C. We tested the hypothesis that a single observation of the ^{1}H NMR spectrum of hyperpolarized ^{13}C formate monitors ^{13}C polarization. Depending on the microwave frequency during the polarization process, in-phase or out-of-phase doublets were observed in the ^{1}H NMR spectrum. Even in this simple two-spin system, ^{13}C polarization was not reflected in the relative area of the J_{CH} doublet components due to strong heteronuclear cross-relaxation. The Solomon equations were used to model the proton signal as a function of time after polarization and to estimate ^{13}C polarization from the ^{1}H NMR spectra.
© 2007 Elsevier Inc. All rights reserved.

Keywords: Dynamic nuclear polarization; Overhauser effect; Solomon equations; Formate; SPINOE

1. Introduction

Polarization enhancement using solid state dynamic nuclear polarization (DNP) followed by rapid dissolution and transport of the hyperpolarized solution to a high field spectrometer has been shown to provide increases in signal to noise for ^{13}C NMR on the order of 10,000 fold or higher [1]. In addition to improved detection of ^{13}C in the hyperpolarized molecule, excess ^{13}C polarization is preserved during metabolism and permits direct ^{13}C imaging of biochemical products such as alanine, lactate, and bicarbonate after hyperpolarization of [1-^{13}C]pyruvate [2–4]. Compared

to radiotracers, NMR detection of ^{13}C offers the overwhelming advantage of monitoring specific metabolic products and for this reason there is now intense interest in developing hyperpolarized ^{13}C-enriched substrates for investigation of biochemical kinetics in vivo [5]. A key component of a quantitative kinetics experiment with hyperpolarized carbon will be determination of the initial ^{13}C polarization achieved by DNP after dissolution. This is performed routinely by comparing signal from an aliquot of the polarized material to a standard solution, but this requires a second functioning NMR spectrometer as well as assumptions regarding the efficient transfer of the sample, the T_1 of the sample in the local fields surrounding it, etc. However, as pointed out in a variety of publications since the 1970s, an estimate of the polarization can be made by measuring the asymmetry in a coupled system [6–10].

---

* Corresponding author.
  E-mail address: matthew.merritt@utsouthwestern.edu (M.E. Merritt).

Using this technique, polarization in a sample of [U–^{13}C, ^{15}N] urea was estimated at 37% by observation of the ^{15}N signal [1]. If this same experiment could be carried out by observing the protons attached to a polarized carbon, the total carbon polarization of a sample could be estimated prior to injection into a subject by sacrificing a few seconds for a ^{1}H NMR observation. A simple and readily polarizable compound for testing this method is [^{13}C]formate. If ^{13}C labeled formate is polarized, the asymmetry of the ^{1}H doublet observed due to $^1J_{CH}$ coupling should be a measure of the ^{13}C polarization achieved. We show here that strong proton–carbon cross-relaxation confounds this measurement if only a single spectrum is acquired. However, if the total proton magnetization is modeled by the Solomon equations as a function of time after ^{13}C polarization, the magnitude of ^{13}C polarization can be inferred [11,12]. Similar SPINOE (Spin Polarization Induced Nuclear Overhauser Effect) type effects have been observed previously for mixtures of noble gases and liquids [13], and on surfaces [14,15], though the magnitude of the Overhauser effect is much smaller in both previous cases since the polarized nuclei are not covalently bonded to other species.

2. Methods

A standard solution of 2.5 M [^{13}C]formate (Cambridge Isotope Laboratories, Andover, MA) was prepared in deionized H_2O. For DNP, 10 μl aliquots of the formate standard were mixed with an equal volume of 15.5 mM trityl radical (tris{8-carboxyl-2,2,6,6-tetra[2-(1-hydroxyethyl)]-benzo(1,2-d:4,5-d′)bis(1,3)dithiole-4-yl}methyl sodium salt) (Oxford Instruments Molecular Biotools Ltd., Oxfordshire, UK) in glycerol. The samples were placed in the 3.35 T Oxford HyperSense (Oxford Instruments Molecular Biotools Ltd., Oxfordshire, UK) DNP system and polarized for 1.5 h prior to dissolution and ejection. The build-up rate constant for the polarization in the solid state was ∼1.5 h. The electron irradiation frequency was set to either 94.118 GHz (positive lobe of DNP enhancement curve) or 94.201 GHz (negative lobe of the enhancement curve) [16]. The sample was held at 1.4 K during the polarization. Dissolution was accomplished by injecting 4 ml of boiling D_2O containing 850 μM EDTA to scavenge any metal ions. Total time of dissolution and ejection of the sample was 5 s. The sample was transferred into an 8 mm outer diameter NMR tube positioned in an INOVA 600 MHz spectrometer (Varian Instruments, Palo Alto, CA) set to begin acquisition when gated externally by the HyperSense. Proton NMR spectra were acquired with an 8 mm inverse detection probe (Nalorac Instruments, Martinez, CA) using a 1° proton pulse followed by a 1 s acquisition time and a 1 s relaxation delay, yielding a time to repeat of 2 s. Each free induction decay was zero-filled to 16,384 points prior to Fourier transformation. The relative peak areas were measured by integration. Direct observation of the ^{13}C signal was also carried out in separate experi-

ments, using a 10 mm broadband Varian probe and a train of 1° excitation pulses. The acquisition time was 1 s with no inter-pulse delay. All parameters regarding the hyperpolarization were held constant for both the ^{1}H and ^{13}C detected experiments. Enhancement of the ^{13}C signal was calculated by comparing the first scan of the experiment to a single pulse spectrum of the thermally polarized sample using a 90° excitation pulse.

2.1. Data analysis

The data was analyzed using programs written within the Matlab (Mathworks, Inc.) computing environment, where the fminsearch algorithm was used to find the minimum least squares difference between simulated decay curves and the data. The integrals for both peaks at each time point were summed and the complete curve was normalized to the value of the integral at the last time point. The total magnetization was simulated using the Solomon equations assuming an inter-nuclear distance of 1.11 Å between the proton and carbon nuclei of formate. The Solomon equations were written in the form shown in Eq. (1):

$$\frac{d}{dt}\begin{pmatrix}\langle I_{HZ}\rangle \\ \langle I_{CZ}\rangle\end{pmatrix} = \begin{pmatrix}-R_{auto} & -R_{cross} \\ -R_{cross} & -R_{auto}\end{pmatrix} * \begin{pmatrix}\langle I_{HZ}\rangle - \langle I_{HZ}\rangle^{eq} \\ \langle I_{CZ}\rangle - \langle I_{CZ}\rangle^{eq}\end{pmatrix}$$

(1)

where $R_{auto} = W_0 + W_H + W_C + W_2$ and $R_{cross} = W_2 - W_0$. The values for the relaxation rates were calculated as follows:

$$W_0 = \frac{1}{10}\left(\frac{\mu_0}{4\pi}\right)^2 \frac{\gamma_H^2 \gamma_C^2 \hbar^2}{r^6}\left(\frac{\tau_C}{1+(\omega_H - \omega_C)^2 \tau_C^2}\right)$$

$$W_H = \frac{3}{20}\left(\frac{\mu_0}{4\pi}\right)^2 \frac{\gamma_H^2 \gamma_C^2 \hbar^2}{r^6}\left(\frac{\tau_C}{1+(\omega_H)^2 \tau_C^2}\right)$$

$$W_C = \frac{3}{20}\left(\frac{\mu_0}{4\pi}\right)^2 \frac{\gamma_H^2 \gamma_C^2 \hbar^2}{r^6}\left(\frac{\tau_C}{1+(\omega_C)^2 \tau_C^2}\right)$$ (2)

$$W_2 = \frac{3}{5}\left(\frac{\mu_0}{4\pi}\right)^2 \frac{\gamma_H^2 \gamma_C^2 \hbar^2}{r^6}\left(\frac{\tau_C}{1+(\omega_H + \omega_C)^2 \tau_C^2}\right)$$

where μ_0 is the permeability of free space, γ_H and γ_C are the gyromagnetic ratios, $\hbar$ is Planck's constant, τ_c is the correlation time, and the ω's are the respective Larmor frequencies. Three parameters were used in the data fitting; the proton, $\langle I_{HZ}\rangle$, polarization, the carbon, $\langle I_{CZ}\rangle$, polarization, and the correlation time (τ_c) for motion of the formate molecule. The values extracted for $\langle I_{HZ}\rangle$ and $\langle I_{CZ}\rangle$ were calculated as a multiplicative factor of the normal Boltzmann population differences (in the high temperature limit), which were defined as:

$$\langle I_Z\rangle = \frac{\hbar\gamma B_0}{2kT}$$

(3)

So a value of 60 for $\langle I_{HZ}\rangle$ indicates a polarization of the proton ensemble 60 times greater than normal for the

14.1 T applied field at 310 K. We do not differentiate between enhancement due to the low temperature versus that gained by the DNP effect alone. Only the dipolar relaxation mechanism was included in the simulations; contributions to relaxation from the chemical shift anisotropy, J-coupling effects, etc. were neglected.

3. Results

A stack plot of a series of ^{1}H spectra of the doublet of [1-^{13}C]formate is shown in the upper panel of Fig. 1. These spectra were obtained following dissolution of a sample polarized with the electron irradiation frequency set to the positive enhancement lobe. The initial ^{1}H signal, acquired 6 s after dissolution, was intense and the ^{1}H signal gained amplitude until approximately 30 s following the dissolution. Subsequently, the ^{1}H signal decayed to steady state at approximately 200 s. The ^{1}H signals of the high frequency (associated with the α state of the ^{13}C) and the low frequency (associated with the β state of the ^{13}C) were antiphase in the first spectrum. By the second time point, both signals had the same phase relative to each other, but opposite of the final phase of the signal observed at equilibrium.
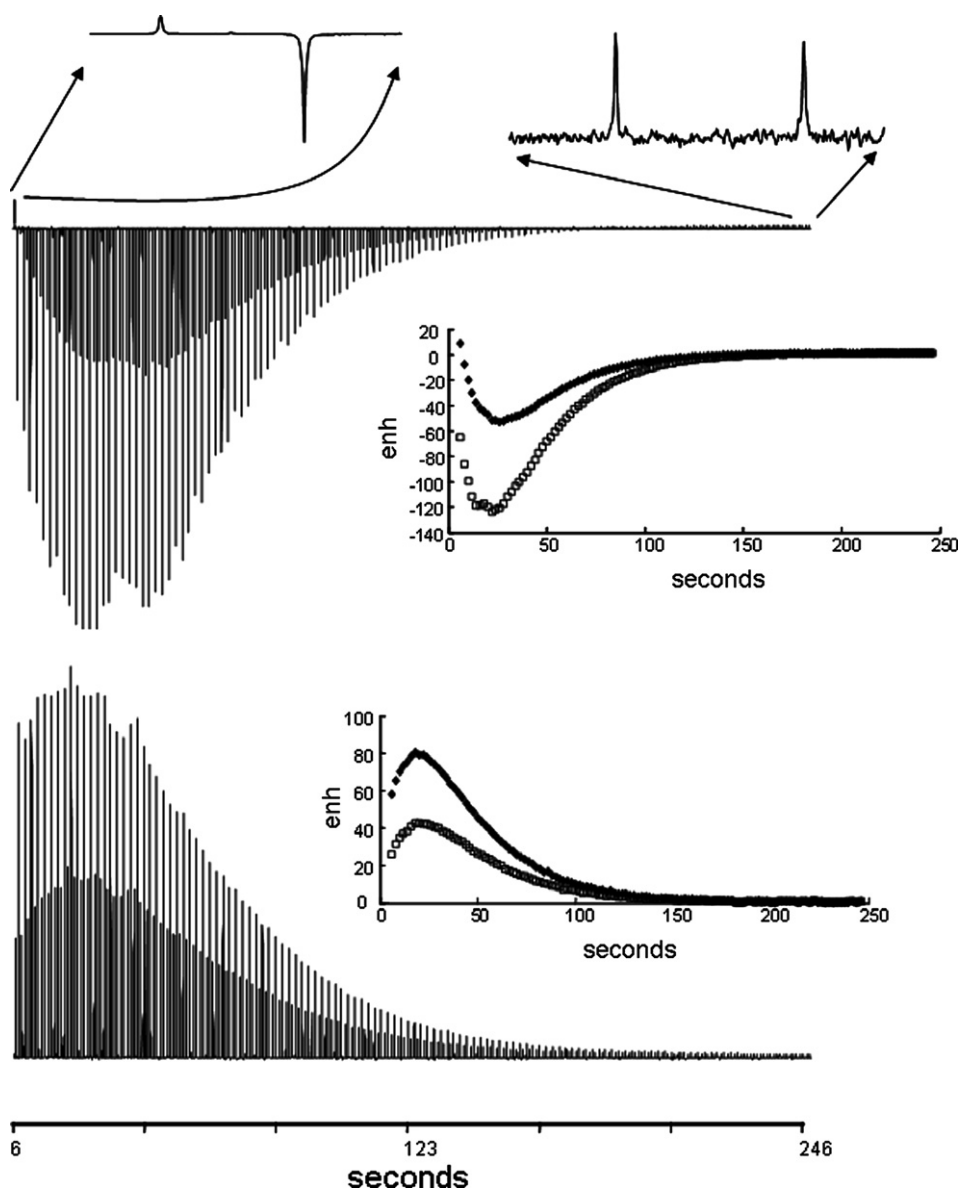

Fig. 1. (Top) Stack plot of the amplitudes for the ^{1}H signal of [1-^{13}C]formate as a function of time following dissolution using polarization on the positive node of the DNP enhancement curve. The upper insets show the ^{1}H NMR signal from the first and last time points. The system returns to equilibrium at approximately 200 s after dissolution. The lower inset shows the time evolution of both peaks in the multiplet (□, downfield peak; ◆, upfield peak). The proton doublet following polarization on the negative enhancement lobe (bottom) does not show the emissive behavior of the other case. Cross-relaxation from the carbons causes the total proton magnetization to increase initially, then decay to thermal equilibrium, at which time the two proton signals return to equal intensity. The inset shows the time evolution for both peaks (□, downfield peak; ◆, upfield peak). The enhancement (enh) is scaled to the thermal polarization.
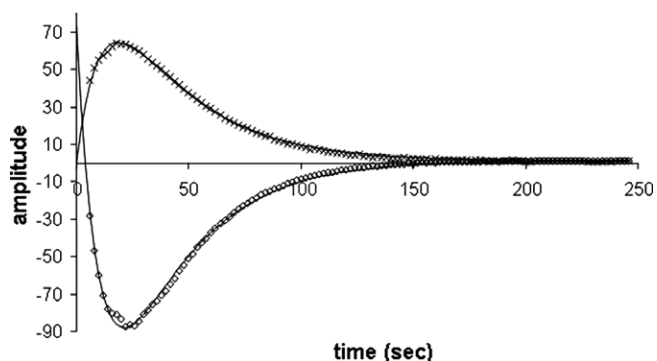
Fig. 2. Measured amplitudes of the total formate proton signal as a function of time following dissolution ($\diamond$, polarized on positive lobe; x, polarized on negative lobe) as recorded with 1° excitation pulses. The solid lines are least squares fits of the data using the Solomon equations. The polarization values extracted from the fit were $\langle I_{HZ} \rangle = 66$ and $\langle I_{CZ} \rangle = 2135$ (for the positive lobe of the enhancement curve) and $\langle I_{HZ} \rangle = -0.27$ and $\langle I_{CZ} \rangle = -1483$ (for the negative lobe).

The effects on the ^{1}H spectrum of polarization on the negative lobe of the DNP enhancement curve are illustrated in the bottom panel of Fig. 1. Under this condition, the two peaks of the doublet had the same phase in the first spectrum. The initial signal was intense, and increased in amplitude until approximately 30 s after dissolution, after which it decayed to the equilibrium value.

Total signal for the protons of formate as a function of time following the dissolution using both experimental conditions is shown in Fig. 2. The fit for the data generated from the enhancement on the positive lobe (Fig. 2, open diamonds) yielded values for $\langle I_{HZ} \rangle$, $\langle I_{CZ} \rangle$, and τ_c of 66 times the thermal equilibrium proton polarization, 2135 times the thermal equilibrium carbon polarization, and 3.32 ps, respectively. As can be seen in the figure, the simulation (solid line) appears to match the functional form of the data exactly. The data from the negative lobe (x's) was also fit, and gave values for $\langle I_{HZ} \rangle$, $\langle I_{CZ} \rangle$, and τ_c of -0.27 times the thermal equilibrium proton polarization, -1483 times the thermal equilibrium carbon polarization, and 3.12 ps. For a series of runs on the positive lobe of the enhancement curve, a value of 1639 ± 356 was obtained. This value can be compared to the average carbon signal enhancement of 2687 ± 710 as measured by direct detection of the ^{13}C signal. These two average values are significantly different at the 95% confidence level (p-value = .02 using a two tailed t-test assuming non-equal variances).

4. Discussion

Clearly, polarization in the carbon pool of formate following dynamic nuclear polarization cannot be determined from the asymmetry within the J-coupled doublet in a single ^{1}H NMR spectrum. The choice of urea as a test compound by Golman and colleagues was ideal since the ^{13}C–^{15}N dipolar coupling is ~10 times weaker than the ^{1}H–^{13}C dipolar coupling in formate. Hence, effects like

those observed here would be much smaller for urea. For formate, strong dipolar relaxation immediately begins to transfer polarization from the ^{13}C spins to the coupled ^{1}H spins upon dissolution. Due to these relaxation effects, the J-coupled doublet in the ^{1}H spectrum can actually have anti-phase intensities, making an estimate of the polarization by the asymmetry difficult without additional information.

The fits to the data using the Solomon equations (Fig. 2, solid line) estimate the different absolute polarizations for the proton and carbon spin baths depending upon whether the DNP was carried out on the positive or negative lobe of the enhancement curve. Two separate observations can be made about these results.

First, total proton polarization depends strongly upon the choice of irradiation frequency for the DNP (either positive or negative enhancement lobe). We believe this phenomenon arises from ^{1}H–^{13}C cross-relaxation in the solid. The carbons and protons are both dipolar and J-coupled in the solid, and hence, as time elapses, the proton spin bath begins to take on the characteristics of the carbon spin bath which is being excited via the DNP interaction. As the carbons polarized on the negative lobe gain "negative polarization", the proton polarization should decrease. It is noteworthy that measurement of the decay of the proton signal without microwave irradiation showed a positive enhancement that could be accounted for by Boltzmann statistics at 1.4 K. It is generally accepted that at this field strength, (3.35 T, or 142.5 MHz proton frequency), the ESR linewidth for the trityl radical is too small to allow for DNP of the proton spin bath directly.

Second, the absolute value of the total carbon polarization is not equivalent between the two runs (Fig. 2), even though the total time for the DNP was held constant at 90 min. This point has a straightforward explanation. For polarization on the negative lobe of the enhancement curve, the initial carbon polarization generated by submerging the sample in a 1.4 K helium bath must be overcome before "negative polarization" can be generated. The solid state NMR analyzer included in the Hypersense system showed a strong initial polarization which disappeared over the first 20 min of microwave irradiation, after which signal began to build again (the solid state measuring system monitors only the absolute amplitude of the signal, so all signals appear positive). Therefore, for a fixed irradiation time as used in these studies, the total carbon polarization developed was less for enhancement on the negative lobe. The build-up time constant for polarization on the negative lobe is equivalent to that of the positive lobe only if the time points following the initial destruction of the polarization are considered.

From a data simulation standpoint, we believe simplification of the simulations to include only dipolar relaxation, while not strictly correct, is a reasonable approximation. The dipolar mechanism is the main source of cross-relaxation between the ^{1}H and ^{13}C. Cross-relaxation caused by J-coupling should be much weaker than that mediated by the

dipolar coupling. Relaxation due to the chemical shift anisotropies would only change the auto-relaxation rates. Modification of the auto-relaxation rates by a factor of two in the simulations resulted in a change of approximately 10% for the total carbon polarization estimated. Given other experimental ambiguities, we judged these errors to be of minimal importance for our initial experiments. Also, the use of 1° excitation pulses means that the net $\langle I_z \rangle$ magnetization is only changing by a very small amount after each individual pulse ($\cos(1°) = 0.9998$). Therefore, the Solomon equations were not modified to include effects of the pulses. One source of error that cannot be accounted for is the sample transfer step through the stray field surrounding the magnets. We do believe transfer from the 3.35 T HyperSense to the 14.1 T NMR magnet is carried out adiabatically since the transport is carried out within the fringe field of one of the magnets at all times. However, at low field, the contribution to relaxation from the W_0 term would increase in magnitude compared to the other terms in the Solomon equations. Simulations indicate this would not cause asymmetries within the proton doublet, but it could confuse the quantitative measurement of the polarization. We believe this is the source of the disagreement between the enhancements measured by this indirect method versus those of direct observation of the hyperpolarized carbon signal.

The explanation of the asymmetry in the proton doublet arises from a more subtle effect. As detailed in Waugh's paper [10], the asymmetry in the J-coupled doublet itself arises from a need to weight the Golden Rule probabilities by the populations of the specified eigenstates (Fig. 3). To
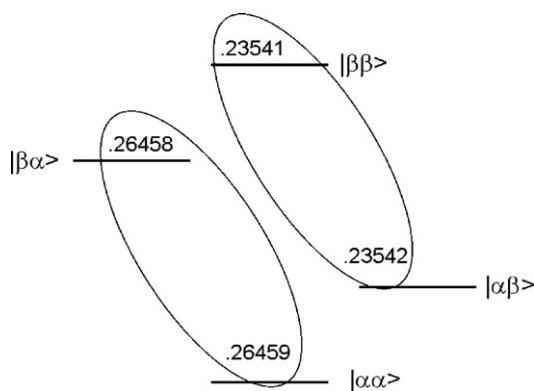
put it plainly, doublets are normally symmetric due to the approximately equal populations of the spins coupled to the observe nucleus, whether they be up or down with respect to the applied field. In the hyperpolarized case, this equality no longer holds and produces the observed asymmetry. It is notable that this effect cannot be accounted for by the definition of $\langle I_z \rangle$, i.e., that $I_z = N^+ - N^-/N^+ + N^-$ where N is the number of spins either up or down. As shown in Fig. 3, at high carbon polarizations and thermal equilibrium proton polarizations, the difference between the proton energy levels, whether it be the $|\alpha\alpha\rangle - |\beta\alpha\rangle$ or the $|\alpha\beta\rangle - |\beta\beta\rangle$ transition remains on the order of the proton polarization and cannot be asymmetric. For this reason, the Solomon equations are insufficient to describe the time dependence of the individual components of the doublet, though they appear sufficient to correctly model the total proton signal. Future work to describe the individual components using a density matrix approach will have to be carried out with Redfield–Bloch theory.

An important benefit of this experiment should be pointed out. The ^{13}C polarization is measured through the protons; no pulses are required on the ^{13}C channel. Similar experiments for measuring the polarization in hyperpolarized xenon by observing a proton chemical shift have previously been reported [17]. This allows the carbon polarization to be indirectly monitored without any perturbation due to destruction of the ^{13}C magnetization by a readout pulse. This is extremely important in removing the effects of mixing in the NMR tube. Four milliliter of solvent is injected rapidly in the 8 mm NMR tube, filling it to nearly four inches of depth. While destruction of the hyperpolarized magnetization can be accounted for [18], the effects of diffusion cannot be easily modeled in tissue. In this case, convection within the sample could easily cause erroneous readings of the polarization if ^{13}C magnetization is being destroyed by a carbon pulse and being replenished by diffusion within the tube. This experiment removes such confounding factors. Assuming a more complete theoretical treatment of the individual components of doublet would give answers that agree with the directly measured carbon enhancements, application of this method could be applied for bolus tracking of a hyperpolarized material in an imaging experiment using a second observe/receive channel set up to detect protons simultaneously, though this was not done here due to hardware limitations on the current system. This type of experiment has previously been performed [19], and indeed, current imaging systems perform simultaneous detection of different frequencies routinely. We believe that this method could be of general importance in future applications when protonated substrates are used; for example, in ^{13}C labeled acetate, a precursor often used to measure Kreb's cycle flux. However, due to uncertainties in the relative contribution of the various relaxation pathways during the transfer step, absolutely quantitative measurements of the total ^{13}C polarization by proton detection is probably precluded without a more advanced theoretical description of the phenomena.

Fig. 3. Populations of the four coupled energy levels of a ^1H–^{13}C spin pair given an arbitrary proton polarization equal to the thermal equilibrium value and a carbon polarization of 10,000 times the thermal equilibrium value. The total population is normalized to 1. Note the total number of spins in the $|\alpha\alpha\rangle - |\beta\alpha\rangle$ (a proton transition) transition is greater than that in the $|\alpha\beta\rangle - |\beta\beta\rangle$ (the other proton transition); this is the source of the asymmetric doublet observed in the spectrum. Also note that the differences that define the $\langle I_{HZ} \rangle$ magnetization from a Solomon perspective are not sufficient to account for the observed spectrum. It is not the differences between the energy levels that explain the doublet asymmetry but rather the total number of spins occupying the respective proton transitions. The values were obtained from direct calculation of the Boltzmann factor without using the high temperature approximation.

Acknowledgments

References

[1] J.H. Ardenkjaer-Larsen, B. Fridlund, A. Gram, G. Hansson, L. Hansson, M.H. Lerche, R. Servin, M. Thaning, K. Golman, Increase in signal-to-noise ratio of >10,000 times in liquid-state NMR, Proceedings of the National Academy of Sciences of the United States of America 100 (18) (2003) 10158–10163.

[2] M. Merritt, C. Harrison, C. Storey, F. M. Jeffrey, A.D. Sherry, C.R. Malloy, Hyperpolarized ^{13}C allows a direct measure of flux through a single enzyme-catalyzed step by NMR, Proceedings of the National Academy of Sciences of the United States of America, in press.

[3] K. Golman, J.H. Ardenkjaer-Larsen, J.S. Petersson, S. Mansson, I. Leunbach, Molecular imaging with endogenous substrates, Proceedings of the National Academy of Sciences of the United States of America 100 (18) (2003) 10435–10439.

[4] K.O. Golman, L.E. Olsson, O. Axelsson, S. Mansson, M. Karlsson, J.S. Petersson, Molecular imaging using hyperpolarized ^{13}C, British Journal of Radiology 76(spec. issue 2) (2003) S118–S127.

[5] K. Golman, R. in't Zandt, M. Thaning, Real time metabolic imaging, Proceedings of the National Academy of Sciences of the United States of America 103 (30) (2006) 11270–11275.

[6] A. Abragam, M. Chapellier, J.F. Jacquinot, M. Goldman, Absorption lineshape of highly polarized nuclear spin systems, Journal of Magnetic Resonance 10 (1973) 322.

[7] C.M. Edwards, D. Zhou, N.S. Sullivan, Unusual low-temperature effects on the NMR line shapes in solid hydrogen, Physical Review B 34 (9) (1986) 6540–6542.

[8] P. Kuhns, O. Gonen, J.S. Waugh, Proton spin–spin and spin–lattice relaxation in $CaSO_4 xH_2O$ below 1 K, Journal of Magnetic Resonance 82 (1989) 231–237.

[9] N.S. Sullivan, R.V. Pound, Nuclear-spin-lattice relaxation of solid hydrogen at low temperatures, Physical Review A 6 (1972) 1102.

[10] J.S. Waugh, O. Gonen, P. Kuhns, Fourier transform NMR at low temperatures, Journal of Chemical Physics 86 (7) (1987) 3816–3818.

[11] I. Solomon, Relaxation processes in a system of two spins, Physical Review 99 (1955) 559–565.

[12] I. Solomon, N. Bloembergen, Nuclear interactions in the HF molecule, Journal of Chemical Physics 25 (1956) 261–266.

[13] G. Navon, Y.Q. Song, T. Room, S. Appelt, R.E. Taylor, A. Pines, Enhancement of solution NMR and MRI with laser-polarized xenon, Science 271 (5257) (1996) 1848–1851.

[14] D. Raftery, E. McNamara, G. Fisher, C.V. Rice, J. Smith, Optical pumping and magic angle spinning: sensitivity and resolution enhancement for surface NMR obtained with laser-polarized xenon, Journal of the American Chemical Society 119 (37) (1997) 8746–8747.

[15] T. Room, S. Appelt, R. Seydoux, Enhancement of surface NMR by laser-polarized noble gases, Physical Review B 55 (17) (1997) 11604–11610.

[16] R.A. Wind, M.J. Duijvestijn, C. Van der Lugt, A. Manenschijn, J. Vriend, Applications of dynamic nuclear polarization in carbon-13 NMR in solids, Progress in Nuclear Magnetic Resonance Spectroscopy 17 (1) (1985) 33–67.

[17] A.S. Verhulst, O. Liivak, M.H. Sherwood, I.L. Chuang, A rapid and precise probe for measurement of liquid xenon polarization, Journal of Magnetic Resonance 155 (2002) 145–149.

[18] B.R. Patyal, J. Gao, R.F. Williams, J. Roby, B. Saam, B.A. Rockwell, R.J. Thomas, D.J. Stolarski, P.T. Fox, Longitudinal relaxation and diffusion measurements using magnetic resonance signals from laser-hyperpolarized ^{129}Xe nuclei, Journal of Magnetic Resonance 126 (1997) 58–65.

[19] O. Gonen, J. Murphy-Boesch, R. Srinivasan, J. Hu, H. Jiang, R. Stoyanova, T.R. Brown, Simultaneous and interleaved multinuclear chemical-shift imaging, a method for concurrent, localized spectroscopy, Journal of Magnetic Resonance, Series B 104 (1) (1994) 26–33.